

ORIGINAL RESEARCH PAPER

Facile Synthesis and Characterization of HNT-Ferrihydrite Nanocomposites for water/wastewater treatment

Syarifah Nazirah Wan Ikhsan^{1,2}, Norhaniza Yusof^{*1,2}, Farhana Aziz^{1,2}, Nurasyikin Misdan³, Ahmad Fauzi Ismail^{*1,2}

¹ Advance Membrane Technology Research Centre (AMTEC), N29A, 81310, Universiti Teknologi Malaysia.

² School of Chemical and Energy Engineering, Faculty of Engineering, 81310, Universiti Teknologi Malaysia.

³ Faculty of Engineering Technology, Universiti Tun Hussein Onn Malaysia, 86400 Parit Raja, Johor, Malaysia.

Received: 2018-07-30

Accepted: 2018-09-23

Published: 2018-10-15

ABSTRACT

In this study, a novel Halloysite nanotube/ferrihydrite (HNT/FH) nanocomposites have been synthesized using simple chemical precipitation method. The prepared nanocomposites were characterized using X-Ray Diffraction (XRD), Fourier Transform Infrared (FTIR) Spectroscopy, Transmission Emission Microscopy (TEM), Energy Dispersive X-Ray Spectroscopy (EDX) and Brunauer–Emmett–Teller (BET). The morphology of the synthesized nanocomposites revealed the attachment of FH to the lining of HNT. XRD patterns revealed the nanocomposite having a monoclinic structure which agrees with the FTIR results. The high surface area of 328.6 m²/g and high aspect ratio of the nanocomposites endowed it with enforcing ability and enhanced water absorption capability, which in turn makes it highly hydrophilic. The high hydrophilic and adsorption ability of the novel nanoparticles has opened a wide opportunity for it to be utilized in the separation of wastewater.

Keywords: Halloysite nanotube-ferrihydrites nanocomposite, Nanocomposite, Nanoparticles, Wastewater Separation

How to cite this article

Wan Ikhsan SN, Yusof N, Aziz F, Misdan N, Fauzi Ismail A. Facile Synthesis and Characterization of HNT-Ferrihydrite Nanocomposites for water/wastewater treatment. J. Water Environ. Nanotechnol., 2018; 3(4): 279-288.

DOI: 10.22090/jwent.2018.04.001

INTRODUCTION

In recent years, attention has been shifted towards the application of nanoparticles as additives in the membrane for treatment of wastewater. The general idea behind the addition of the nanoscale second phase is to create synergy between the various constituents, such that novel properties capable of meeting or exceeding design expectations can be achieved [1].

The aim of fabricating a composite is to combine materials with the objective of getting a more desirable combination of properties. The properties of nanocomposites rely on a range of variables, particularly the matrix material, which can exhibit nanoscale dimensions, loading, the

degree of dispersion, size, shape, and orientation of the nanoscale second phase and interactions between the matrix and the second phase [2]. The structure of nanocomposites usually consists of the matrix material containing the nanosized reinforcement components in the form of particles, whiskers, fibers, nanotubes, etc [3]. Expanding nanocomposite has been demonstrated to exhibit collaborations with contaminants in water, gases and even soil and such properties open opportunity for new and enhanced ecological innovation [4]. Nonetheless, small sized molecule likewise brings issues such mass transport and inordinate flux drop at whatever point connected in flow-through frameworks and additionally certain problems in separation and reuse, and even conceivable hazard

* Corresponding Author Email: norhaniza@petroleum.utm.my
afauzi@utm.my

to biological communities and human well-being caused by the potential release of nanoparticles [5]. A compelling way to deal with the previously mentioned bottlenecks is to manufacture hybrid nanocomposite by grafting or coating the fine particles onto strong particles of bigger size [6].

Nanocomposites are often being chosen in most of the application due to its nanoparticles properties that bring about different enhancements to the matrix, its multifunctional abilities which comes from its different constituents, the broad chemical functionalization which made it tuneable to suits any environment or applications, and its huge interphase zone that allow more modification [7, 8]. In the field of nanocomposites, many diverse topics exist including composite reinforcement, barrier properties, flame resistance, electro-optical properties, cosmetic applications, bactericidal properties [9]. Numerous studies regarding the utilization of nanocomposite have been explored towards the wastewater treatments application. For instance, Ahmad and his co-worker have developed PSF membrane functionalized by blending SiO₂ nanocomposite to enhance the hydrophobicity of the membrane. The study resulted in improved permeate flux of the SiO₂ embedded membrane from 1.08L/m²h to 17.32L/m²h. Additionally, they also found that increasing the nanocomposite load has concurrently increased the membrane's antifouling properties.

Additionally, several studies have reported that the incorporation of nanoparticles such as GO[10–13], TiO₂[14–17], Fe₃O₄[18–20], and clay[21–23] onto polymers could not only adjust the structure and physicochemical properties which include changing the hydrophilicity, porosity, charge density, chemical, thermal and mechanical stability of membranes, but institute distinctive properties such as antibacterial and antifouling properties into the membranes.

Among commonly used nanoparticles, halloysite nanotube (HNT) has emerged as one of the efficient additives for membrane incorporation. It possessed championed characteristics such as fine particle, high surface area, excellent dispersion as well as great cation exchange capacity and has the ability to maintain uniform shape, sustained release rates and no initial over dosage[24]. Since HNT has the ability to be tuned accordingly, there is a possibility to increase the uptake of -OH group by increasing the absorption capabilities of the composite. This absorption capability can be enhanced by coupling

HNT with absorptive materials such as Ferrihydrites (FH). Ferrihydrites (FH) is an efficient sorbent for inorganic and organic pollutants and therefore have great potentials in environmental science and engineering applications [25]. Because of its properties as an effective sorbent for numerous inorganic and organic pollutants in soils and water, FH plays a key role in pollution abatement of contaminated soils, water treatment technology, and the metal and mining industries.

Therefore, with the motivation to the couple, the novel HNT-FH to increase the water absorption capabilities, in this study, a thorough discussion of facile synthesis of HNT-FH nanocomposite will be provided. The novel nanocomposites were characterized for its morphological and physicochemical properties with various characterization machines to evaluate its properties.

MATERIALS

Ferric chloride hexahydrate (FeCl₃·6H₂O), hydrochloric acid (HCl), ammonia solution (NH₄OH), halloysite nanotube nanopowder supplied by Sigma Aldrich has been used for synthesizing HNT-FH nanocomposite. For fabrication of nanocomposite-embedded membrane, commercial PES pellets (Ultrason®E) purchased from BASF SE Germany is the main component in membrane formation. Dimethylacetate (DMAc) and polyvinylpyrrolidone (MW=24,000 g/mol) supplied by Merck has been used as a polymer solution and pore forming agent. For wastewater treatment analysis, the wastewater was collected from the cafeteria in Universiti Teknologi Malaysia (UTM), Johor, Malaysia.

EXPERIMENTALS

Synthesis of HNT-FH nanoparticles

The synthesis of HNT-FH initially started with the preparation of FH precursor by adding 0.205 mL of 0.01M HCl in 250 mL of deionized water. This has been followed by addition of 1.0M ferric chloride hexahydrate (FeCl₃·6H₂O) as a precursor, approximately 67.75gm into HCl dilute solution. The precursor solution of FH was maintained at 65 °C. Then, 0.5 g of HNTs were added to the precursor solution under constant stirring. The pH of the solutions is kept at 7 by addition of ammonium solution. The precipitates then separated from the matrix to obtain the resultant nanocomposite [26]. Finally, the HNT-FH precipitate was rinsed with distilled water and left to age for a week at ambient temperature before filtration and drying at 65 °C.

The dried nanocomposite was then grinded into powder for further testing.

Characterization of HNT-FH nanocomposite

Fourier-transform infrared (FTIR) spectra of the samples were recorded with a Fourier-transform infrared spectrometer (Thermo, Madison, USA) in the wavenumber range from 4000 cm^{-1} to 500 cm^{-1} using KBr pellets. Powder X-ray diffraction (XRD) data were collected using a Rigaku D/max-rA X-ray. The morphologies and sizes of the nanocomposite were observed using a high-resolution transmission electron microscope (TEM) (Model: HT 7700, Hitachi). Brunauer–Emmett–Teller (BET) analysis was conducted with a specific area and pore analyzer (NOVA 2200e, Quantachrome, USA). The elemental mapping of the nanoparticles and the membrane has been done by Energy Dispersive X-Ray (EDX) analysis (Model: TM 3000, Hitachi).

Performance analysis of HNT-FH nanocomposite

The HNT-FH nanocomposite was analyzed for its performance in terms of water uptake ability as well as water flux by incorporating the nanocomposite into PES membrane. Pure water permeation flux (PWP) of membranes was obtained using dead-end tubular UF using the method proposed by Tseng, Zhuang, and Su (2012) [27]. Before pure water flux estimation, the cut membrane inside the cell was initially pressurized with distilled water at 101.32 kPa for 30 min and was then used in subsequent pure water flux estimation experiments at 68.95 kPa for 2 h. The water uptake test of the nanocomposite-incorporated membrane was carried out by employing a method reported by Wang et al., (2002) [28]. The membranes were vacuum-dried at 100 °C for 24 h, weighed and immersed in deionized water at room temperature for 24 h. The wet membranes were wiped dry and quickly weighed again. The water uptake of membranes is reported in weight percent as follows:

$$\text{Water uptake} = \frac{W_{\text{wet}} - W_{\text{dry}}}{W_{\text{dry}}} \times 100$$

Where W_{wet} and W_{dry} are the weights of the wet and dry membranes respectively.

PES-HNT/FH membrane fabrication for wastewater separation analysis

Fabrication of PES/HNT-HFO flat sheet MMMs is also based on the method explained by Abdullah,

et al., 2016 [29]. First, the uniform suspension that has been prepared is poured onto a smooth glass plate and cast by a casting blade at a speed of 5 cm s^{-1} in order to form a film with 250 μm thickness. Then, the cast film is immersed into DI water bath together with the glass plate for a few minutes. This step will allow the phase inversion to take place. The membrane is then transferred to another water bath once it is peeled off naturally from the glass plate. The membrane is left in the water bath for 3 days to ensure complete removal of residual solvent and PVP. The membrane is then dried at ambient temperature (with humidity between 60 and 70%) before using.

The cross-flow UF study has been carried out using the method used by Gohari et al. (2014) [30]. The permeates has been sampled every 10 min for the course of 2 h. The specific end goal of this test is to assess the impact of wastewater concentration and on the permeate flux and foulant dismissal of membranes. The equation used to determine the PWP flux has been used to determine the permeate flux when the membrane is used to treat the synthetic oil emulsions. To decide the dismissal of the membrane against the wastewater at various feed conditions, the accompanying condition was utilized [31]

$$R\% = \left(1 - \frac{C_p}{C_f}\right) \times 100$$

Where R% is the membrane rejection ratio, C_p (mg/L) is the permeate concentration and C_f (mg/L) is the feed concentration. Then, the oil concentration of samples is analyzed using UV-vis spectrophotometer at 305 nm.

RESULTS

Morphological properties of HNT-FH nanocomposite

The morphological studies of the magnetic halloysite-iron oxide nanocomposite were performed using transmission electron microscope (TEM). In Fig. 1, HNT was attached with clusters of FH. FH nanoparticle aggregates were composed of even smaller subunits of about 10 nm, implying that the smaller nanoparticles formed first and then agglomerated around the nanotubes. The appearance of tubes can be observed at the edge of the nanocomposite and FH agglomerates were found around the nanotube as indicated by the red circle. Since FH is slightly magnetic, it is difficult to acquire a stable image to depict the attachment of FH on the HNT.

PHYSICOCHEMICAL ANALYSIS OF HNT-FH NANOCOMPOSITE

Functional group analysis

In this study, attenuated total reflectance Fourier transform infrared (ATR-FTIR) showing the functional groups of the nanocomposites as well as the Mixed Matrix Membrane. Fig. 2 shows the ATR-FTIR graphs of all mix matrix membrane in comparison to pristine PES membrane. In the FTIR spectrum of HNT-FH absorption bands at 701 and 3628 cm^{-1} are ascribed to -OH groups. The band at 910 cm^{-1} is assigned to the bending vibration of Al-OH. Other bands at 1000–1100 and 450–550 cm^{-1} are due to the Si-O stretching and Si-O bending vibrations, respectively [32]. In addition to that, peaks found at the range of 1200 to 1300 cm^{-1} , 1400 to 1500 cm^{-1} , 1600 to 1800 cm^{-1} and 3000 to 3500 cm^{-1} corresponded to Fe-O, O=C=O

stretching, O-H bending and stretching vibrations, respectively[33].

Energy dispersive X-ray (EDX) analysis further reveals the presence of carbon and nitrogen along with the three main constituents, oxygen, aluminum, and silicon in HNT-FH, signifying the functionalization of FH onto HNTs. The EDX analysis is as shown in Fig. 3.

Further analysis of the nanocomposite composition done through XRD analysis. Fig 4 shows the XRD pattern of the HNT-FH nanocomposite. The typical diffraction peaks of halloysite are located at $2\theta = 24.8^\circ$ [34] and the diffraction peaks located at $2\theta = 33.34, 34.65^\circ$ represent the typical peaks for FH [29]. All the typical peaks can be found in the XRD pattern of the synthesized HNT-FH as shown in fig 3. All other sequential peaks at $40.801^\circ, 49.426^\circ, \text{ and } 53.988^\circ$

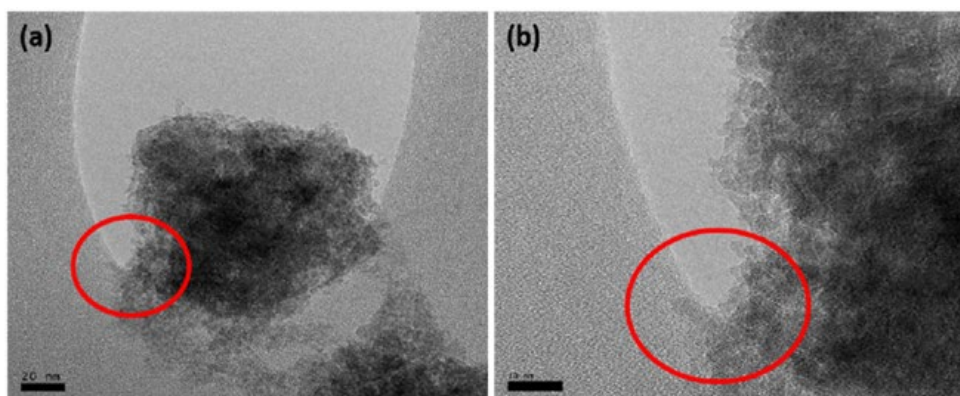


Fig. 1. TEM micrograph of HNT-FH at different scale bar (a) 20nm and (b) 10 nm

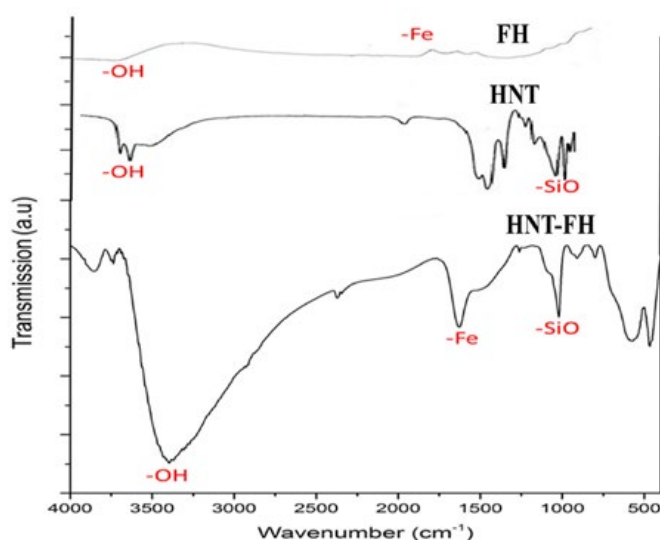


Fig. 2. FTIR spectra of FH, HNT, and FH-HNT nanocomposite

are matched to iron oxide peaks which denote the higher presence of FH which is aligned with the synthesizing ratio of HNT-FH as mentioned in the previous part.

Adsorption and surface charges analysis

Further analysis of the adsorption isotherm of HNT-FH was done through BET analysis. The surface area of the HNT-FH nanoparticles is calculated to be 328.6 m²/g in terms of BET surface area. In comparison to the FH surface area obtained from our previous work which is 233.5 m²/g[8], that indicated the nanocomposites have 140.7% higher surface area which proved that the addition of HNT has increased the surface area of the nanocomposite.

In order to better understand the mechanics behind the nanocomposite surface interactions, the zeta potential measurements were carried out to evaluate the surface charges of HNT, FH, and HNT-FH particles separately. From the analysis, it was found that HNT has a negative charge which is in accordance with the study done by Hu et al., (2016)[35]. High electronegativity promotes the attachment of the positive charge water molecules which in turn contribute to the increased hydrophilicity of the modified membrane incorporated with HNT-FH. All of the zeta potential analyses were carried out at constant pH of 7. HNT recorded average zeta potential of -14.3mV, FH at 27.3mV and the nanocomposite HNT-FH recorded the zeta potential of 21.6mV. Nanoparticles with zeta potential values of 20 to

30 mV are moderately stable at which the stability depends on the Van der Waals attractive forces and electrostatic repulsive due to adsorbed double layer (EDL)[36, 37]

This increased surface area has affected the membrane hydrophilicity as it simultaneously increased the water absorption area[38–40]as well as frequent oil spill accidents. We report in this work the fabrication of a zwitterionic polyelectrolyte brush (poly(3-(N-2- methacryloxyethyl-N,N-dimethyl. The analysis of the nanoparticles isotherm has shown that HNT-FH nanocomposites had resulted in type II isotherm in which it is macroporous with pore diameters more than 50nm and flat surface with uniform surface energy [41]. The results show that the nanocomposite adsorption isotherm exhibited massive deviation from the Langmuir model of adsorption principally owing to active heterogeneities of the nanocomposite surface as well as to the molecular interfaces. As shown in Fig. 4, it can be seen that the intermediate flat region in the isotherm corresponds to monolayer formation. In Fig. 5, the existence of mesopores can be pointed towards the lagging amongst the adsorption and desorption branch [42].

PERFORMANCE ANALYSIS OF HNT-FH

Water uptake analysis

The water uptake analysis of the membrane provides critical insight into how the embedded of nanocomposite can help in enhancing the hydrophilicity of the membrane. Fig. 6 illustrated the static contact angle of the membrane as well as

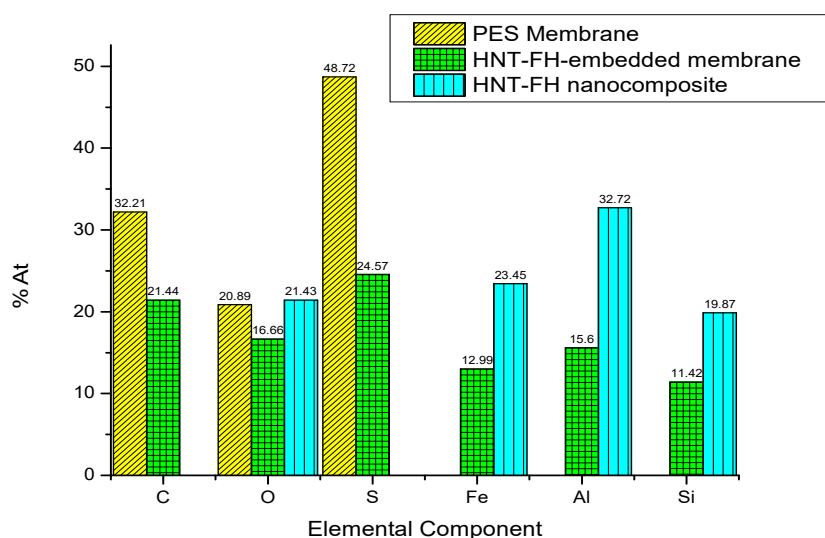


Fig. 3. EDX Elemental component of pristine PES membrane, nanocomposite-embedded membrane, and HNT-FH nanocomposite

the ones embedded with different nanoparticles. It was observed that the membrane incorporated with HNT-FH recorded the lowest static contact angle but the highest water uptake. In comparison

to pristine membrane and membrane incorporated by only HNT and FH, respectively, a significant increase of the hydrophilicity can be seen by the momentous differences between contact angle and

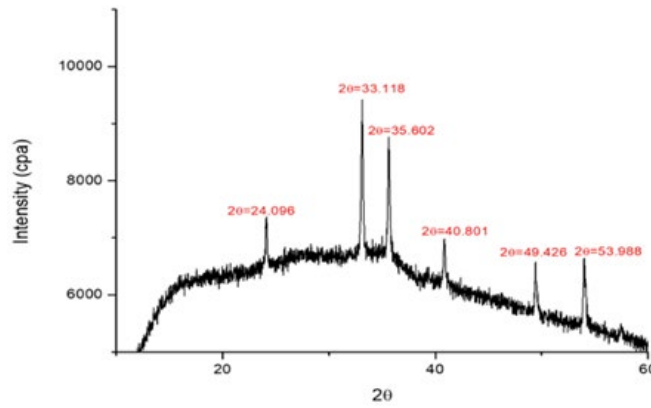


Fig. 4. XRD Patterns of HNT-FH nanocomposite

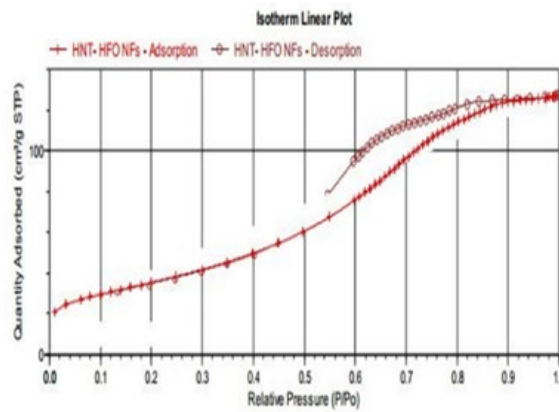


Fig. 5. Isotherm linear plot of HNT-FH nanocomposite

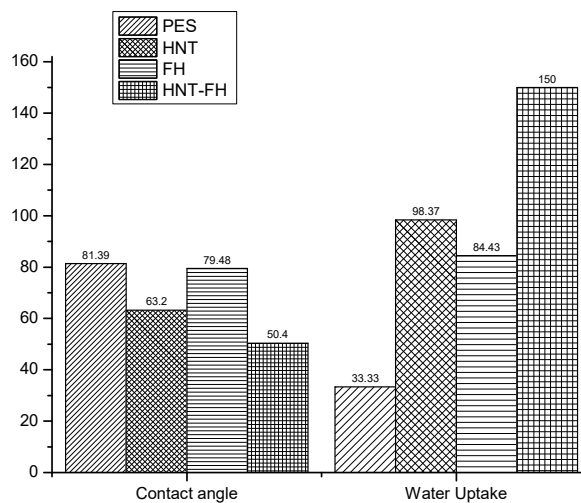


Fig. 6 Static contact angle and water uptake of membrane-embedded with different nanoparticles.

water uptake percentage of the membrane.

The contact angle of PES neat membrane and the modified membranes with different nanoparticles embedded in it has a significant difference as depicted in Fig. 6. As depicted, it can be seen that the contact angle of the membrane with HNT-FH is the lowest with only 50.4° in comparison with pristine PES membrane which is 81.39°. Both HNT and FH embedded membrane shown higher contact angle in comparison with neat PES but still higher than a membrane with HNT-FH nanocomposite. The water uptake ability of the membrane also recorded the highest with HNT-FH nanocomposite as an additive and shows more than five-fold increase in comparison with the neat membrane. This results showed that the addition of HNT-FH into membrane has significantly amplified the membrane contact angle and water uptake capability which reflected the membrane excellent hydrophilicity and water permeability.

Water Flux Analysis

As shown in Fig. 7, the pure water flux of the membrane embedded with HNT-FH recorded the highest which is 642.86 L/m²h. The water flux of the membrane incorporated with HNT-FH

nanocomposite increased to more than two-fold as compared to pristine PES membrane which is 63.57 Lm⁻²h⁻¹. A membrane with only HNT and FH also shown increased water flux with 106.45 L/m²h and 87.55 L/m²h, respectively. The significant increase in water flux of the membrane with HNT-FH nanocomposite are owed to this is due to the abundant -OH group from the HNT-FH nanocomposites as confirmed by FTIR analysis depicted in Fig. 2. This was attributed to more water absorption hence increased hydrophilicity. The water flux of the HNT-FH incorporated membrane can be observed to be relatively higher in comparison to another nanocomposite membrane. Table 1 listed the comparison of HNT-FH incorporated membrane with another nanocomposite membrane. It can be seen that HNT-FH membrane recorded the highest pure water flux with over ten-fold differences in comparison with another membrane.

The HNT-FH incorporated membrane was further analyzed for its performance in the treatment of wastewater. The pure water flux experiment was repeated by replacing the feed with wastewater acquired from the local cafeteria. Wastewater from food and beverages industry often composed of

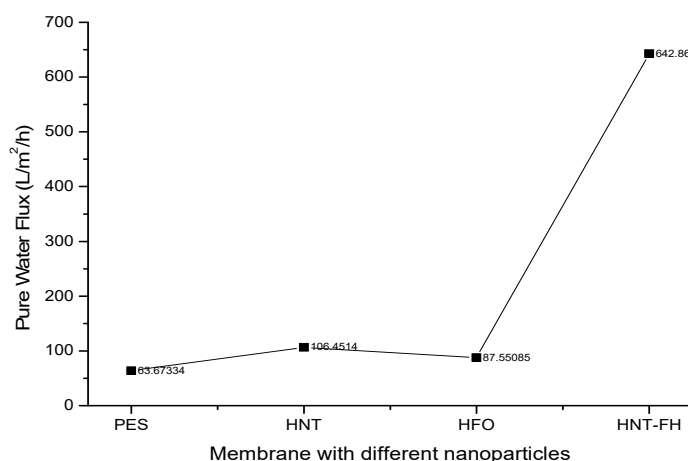


Fig. 7. Pure Water flux of different membrane embedded with HNT-FH and nanocomposite HNT-FH

Table 1. Pure Water Flux (L/m²h) of membrane incorporated with different nanocomposite

Membrane	Pure Water Flux (L/m ² h)	Author
HNT-FH/PES	642.86	This study
HMO/PES	573.2	[30]
coNP/PES	257.79	[43]
GO/PES	20.4	[10]
TiO ₂ /PES	7.2	[44]
ITO/PES	3.0	[45]



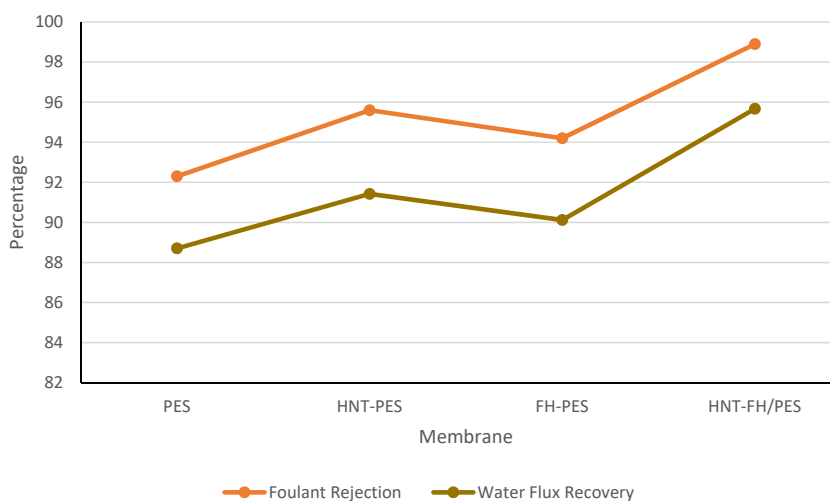


Fig. 8. Foulant rejection (%) and water flux recovery percentage of membrane incorporated with different nanoparticles

a different component, mainly grease and an oily substance. Therefore, membrane hydrophilicity is important to achieve high separation of these materials. Fig. 8 depicted the foulant rejection of the membrane with the wastewater as feed. It can be seen that membrane incorporated with HNT-FH nanocomposite recorded the highest rejection of foulant with significantly higher water flux recovery after the wastewater sample analysis. Pristine PES membrane shows only 88% water flux recovery as opposed to HNT-FH incorporated membrane with 95% water flux recovery after the wastewater treatment analysis which indicated that incorporation of HNT-FH nanocomposite has substantially increased in the water permeability of the membrane even after treatment of the wastewater.

CONCLUSION

In the present study, halloysite nanotube-Ferrihydrites (HNT-FH) were synthesized and characterized by hydrophilic properties. FTIR and TEM images of the synthesized nanocomposites confirmed the attachment of FH to the surface of HNT. large pore volume and high surface of HNT-FH was concluded from BET whereas the obtained result from the XRD that the abundance of -OH group has endowed the nanocomposite with enhanced ability for water absorbency making it suitable to be applied in treatment of oily wastewater and the surface charge analysis of the nanocomposite had proven the capability of nanocomposite in enhancing the hydrophilicity

and antifouling properties due to its electrophoretic mobility, steric barrier as well as agglomeration inhibition.

ACKNOWLEDGMENT

The author would like to express their gratitude for the support and funds by Ministry of Higher Education (MOHE) Malaysia through Fundamental Research Grant Scheme (R.J130000.7846.4F929), GUP grant (Q.J130000.2546.16H29), and Higher Institution Centre of Excellence (HiCOE) grant (R.J090301.7846.4J180 and (R.J090301.7846.4J179).

REFERENCES

1. Gangopadhyay R, De A. Conducting Polymer Nanocomposites: A Brief Overview. *Chemistry of Materials*. 2000;12(3):608-22.
2. Pokropivnyi V. (2002) Two-Dimensional Nanocomposites: Photonic Crystals and Nanomembranes (Review). Part 1. Types and Preparation. *Powder Metall Met Ceram* 41:264-272.
3. Fischer H. Polymer nanocomposites: from fundamental research to specific applications. *Materials Science and Engineering: C*. 2003;23(6-8):763-72.
4. Klefenz H. *Nanobiotechnology: From Molecules to Systems. Engineering in Life Sciences*. 2004;4(3):211-8.
5. Zhang W (2003) Nanoscale Iron Particles for Environmental Remediation: An Overview. *J Nanoparticle Res* 5:323-332. doi: 10.1023/A:1025520116015
6. Zhao X, Lv L, Pan B, Zhang W, Zhang S, Zhang Q. Polymer-supported nanocomposites for environmental application: A review. *Chemical Engineering Journal*. 2011;170(2-3):381-94.
7. Paul DR, Robeson LM. Polymer nanotechnology: Nanocomposites. *Polymer*. 2008;49(15):3187-204.

8. Ouyang C-F, Gong B, Gao Q. Nanocomposite Reinforcement Effects in Millable Polyurethane Elastomer with Low Content of Halloysite Nanotubes. Proceedings of the 2015 International Conference on Material Science and Applications: Atlantis Press; 2015.
9. Thostenson E, Li C, Chou T. Nanocomposites in context. Composites Science and Technology. 2005;65(3-4):491-516.
10. Zinadini S, Zinatizadeh AA, Rahimi M, Vatanpour V, Zangeneh H. Preparation of a novel antifouling mixed matrix PES membrane by embedding graphene oxide nanoplates. Journal of Membrane Science. 2014;453:292-301.
11. Kumar M, Gholamvand Z, Morrissey A, Nolan K, Ulbricht M, Lawler J. Preparation and characterization of low fouling novel hybrid ultrafiltration membranes based on the blends of GO-TiO₂ nanocomposite and polysulfone for humic acid removal. Journal of Membrane Science. 2016;506:38-49.
12. Crock CA, Rogensues AR, Shan W, Tarabara VV. Polymer nanocomposites with graphene-based hierarchical fillers as materials for multifunctional water treatment membranes. Water Research. 2013;47(12):3984-96.
13. Ganesh BM, Isloor AM, Ismail AF. Enhanced hydrophilicity and salt rejection study of graphene oxide-polysulfone mixed matrix membrane. Desalination. 2013;313:199-207.
14. Yang Y, Zhang H, Wang P, Zheng Q, Li J. The influence of nano-sized TiO₂ fillers on the morphologies and properties of PSF UF membrane. Journal of Membrane Science. 2007;288(1-2):231-8.
15. Ai L, Zhou Y, Jiang J. Removal of methylene blue from aqueous solution by montmorillonite/CoFe₂O₄ composite with magnetic separation performance. Desalination. 2011;266(1-3):72-7.
16. Soltani RDC, Safari M, maleki A, Rezaee R, Teymouri P, Hashemi SE, et al. Correction to: Preparation of Chitosan/ Bone Char/Fe₃O₄ Nanocomposite for Adsorption of Hexavalent Chromium in Aquatic Environments. Arabian Journal for Science and Engineering. 2018;43(11):6665-.
17. Bae T-H, Tak T-M. Effect of TiO₂ nanoparticles on fouling mitigation of ultrafiltration membranes for activated sludge filtration. Journal of Membrane Science. 2005;249(1-2):1-8.
18. Gholami A, Moghadassi AR, Hosseini SM, Shabani S, Gholami F. Preparation and characterization of polyvinyl chloride based nanocomposite nanofiltration-membrane modified by iron oxide nanoparticles for lead removal from water. Journal of Industrial and Engineering Chemistry. 2014;20(4):1517-22.
19. Daraei P, Madaeni SS, Ghaemi N, Khadivi MA, Astinchap B, Moradian R. Fouling resistant mixed matrix polyethersulfone membranes blended with magnetic nanoparticles: Study of magnetic field induced casting. Separation and Purification Technology. 2013;109:111-21.
20. Abass O A, Jameel AT, Muyubi SA, Abdul Karim MI, Alam, Md Z. Removal of Oil and Grease as Emerging Pollutants of Concern (EPC) in Wastewater Stream. IIUM Engineering Journal. 1970;12(4).
21. Ma Y, Shi F, Zhao W, Wu M, Zhang J, Ma J, et al. Preparation and characterization of PSf/clay nanocomposite membranes with LiCl as a pore forming additive. Desalination. 2012;303:39-47.
22. Lai CY, Groth A, Gray S, Duke M. Investigation of the dispersion of nanoclays into PVDF for enhancement of physical membrane properties. Desalination and Water Treatment. 2011;34(1-3):251-6.
23. Lai CY, Groth A, Gray S, Duke M. Enhanced abrasion resistant PVDF/nanoclay hollow fibre composite membranes for water treatment. Journal of Membrane Science. 2014;449:146-57.
24. Berahman R, Raiati M, Mehrabi Mazidi M, Paran SMR. Preparation and characterization of vulcanized silicone rubber/halloysite nanotube nanocomposites: Effect of matrix hardness and HNT content. Materials & Design. 2016;104:333-45.
25. Streat M, Hellgardt K, Newton NLR. Hydrous ferric oxide as an adsorbent in water treatment. Process Safety and Environmental Protection. 2008;86(1):11-20.
26. Milkovič O, Janák G, Nižnik Š, Longauer S, Fröhlich L. Iron nanoparticles produced by precipitation phenomena in solid state. Materials Letters. 2010;64(2):144-6.
27. Tseng H-H, Zhuang G-L, Su Y-C. The effect of blending ratio on the compatibility, morphology, thermal behavior and pure water permeation of asymmetric CAP/PVDF membranes. Desalination. 2012;284:269-78.
28. Wang F, Hickner M, Kim YS, Zawodzinski TA, McGrath JE. Direct polymerization of sulfonated poly(arylene ether sulfone) random (statistical) copolymers: candidates for new proton exchange membranes. Journal of Membrane Science. 2002;197(1-2):231-42.
29. Abdullah N, Gohari RJ, Yusof N, Ismail AF, Juhana J, Lau WJ, et al. Polysulfone/hydrous ferric oxide ultrafiltration mixed matrix membrane: Preparation, characterization and its adsorptive removal of lead (II) from aqueous solution. Chemical Engineering Journal. 2016;289:28-37.
30. Jamshidi Gohari R, Halakoo E, Lau WJ, Kassim MA, Matsuura T, Ismail AF. Novel polyethersulfone (PES)/hydrous manganese dioxide (HMO) mixed matrix membranes with improved anti-fouling properties for oily wastewater treatment process. RSC Adv. 2014;4(34):17587-96.
31. Liu G-h, Ye Z, Tong K, Zhang Y-h. Biotreatment of heavy oil wastewater by combined upflow anaerobic sludge blanket and immobilized biological aerated filter in a pilot-scale test. Biochemical Engineering Journal. 2013;72:48-53.
32. Tierrablanca E, Romero-García J, Roman P, Cruz-Silva R. Biomimetic polymerization of aniline using hematin supported on halloysite nanotubes. Applied Catalysis A: General. 2010;381(1-2):267-73.
33. Hsieh S, Huang BY, Hsieh SL, Wu CC, Wu CH, Lin PY, et al. Green fabrication of agar-conjugated Fe₃O₄magnetic nanoparticles. Nanotechnology. 2010;21(44):445601.
34. Zhang A, Mu B, Luo Z, Wang A. Bright blue halloysite/CoAl₂O₄ hybrid pigments: Preparation, characterization and application in water-based painting. Dyes and Pigments. 2017;139:473-81.
35. Hu D, Zhong B, Jia Z, Lin J, Liu M, Luo Y, et al. A novel hybrid filler of halloysite nanotubes/silica fabricated by electrostatic self-assembly. Materials Letters. 2017;188:327-30.
36. Agrawal YK, Patel V. Nanosuspension: An approach to enhance solubility of drugs. Journal of Advanced Pharmaceutical Technology & Research. 2011;2(2):81.
37. Missana T, Adell A. On the Applicability of DLVO Theory to the Prediction of Clay Colloids Stability. Journal of Colloid and Interface Science. 2000;230(1):150-6.
38. Zhu Y, Zhang F, Wang D, Pei XF, Zhang W, Jin J. A

- novel zwitterionic polyelectrolyte grafted PVDF membrane for thoroughly separating oil from water with ultrahigh efficiency. *Journal of Materials Chemistry A*. 2013;1(18):5758.
39. Su Y, Li C, Zhao W, Shi Q, Wang H, Jiang Z, et al. Modification of polyethersulfone ultrafiltration membranes with phosphorylcholine copolymer can remarkably improve the antifouling and permeation properties. *Journal of Membrane Science*. 2008;322(1):171-7.
 40. Hester JF, Banerjee P, Mayes AM. Preparation of Protein-Resistant Surfaces on Poly(vinylidene fluoride) Membranes via Surface Segregation. *Macromolecules*. 1999;32(5):1643-50.
 41. Lowell S, Shields JE (1984) Powder Surface Area and Porosity. In: *Powder Surface Area and Porosity*. Springer Netherlands, Dordrecht, pp 11–13
 42. Keller JU, Staudt R (2005) Adsorption Isotherm. In: *Gas Adsorption Equilibria*. Springer US, Boston, pp 359–413
 43. Gzara L, Ahmad Rehan Z, Khan SB, Alamry KA, Albeirutty MH, El-Shahawi MS, et al. Preparation and characterization of PES-cobalt nanocomposite membranes with enhanced anti-fouling properties and performances. *Journal of the Taiwan Institute of Chemical Engineers*. 2016;65:405-19.
 44. Vatanpour V, Madaeni SS, Moradian R, Zinadini S, Astinchap B. Novel antibifouling nanofiltration polyethersulfone membrane fabricated from embedding TiO₂ coated multiwalled carbon nanotubes. *Separation and Purification Technology*. 2012;90:69-82.
 45. Khorshidi B, Hajinasiri J, Ma G, Bhattacharjee S, Sadrzadeh M. Thermally resistant and electrically conductive PES/ITO nanocomposite membrane. *Journal of Membrane Science*. 2016;500:151-60.